JOURNAL OF VIROLOGY, June 1994, p. 3478–3485
0022-538X/94/$04.00+0

Vol. 68, No. 6

Requirement of Human Immunodeficiency Virus Type 1 *nef* for In Vivo Replication and Pathogenicity

BETH D. JAMIESON,[1] GRACE M. ALDROVANDI,[1] VICENTE PLANELLES,[1] JEREMY B. M. JOWETT,[1] LIANYING GAO,[1] LILLIAN M. BLOCH,[1] IRVIN S. Y. CHEN,[2] AND JEROME A. ZACK[1]*

Division of Hematology-Oncology, Department of Medicine,[1] and Department of Microbiology & Immunology,[2] UCLA School of Medicine and Jonsson Comprehensive Cancer Center, Los Angeles, California 90024-1678

Received 17 December 1993/Accepted 17 February 1994

The role of human immunodeficiency virus type 1 (HIV-1) accessory genes in pathogenesis has remained unclear because of the lack of a suitable in vivo model. The most controversial of these genes is *nef*. We investigated the requirement for Nef for in vivo replication and pathogenicity of two isolates of HIV-1 (HIV-1_{JR-CSF} and HIV-1_{NL4-3}) in human fetal thymus and liver implants in severe combined immunodeficient mice. HIV-1_{JR-CSF} and HIV-1_{NL4-3} differ in their in vitro phenotypes in that HIV-1_{JR-CSF} does not induce syncytia and is relatively noncytopathic, while HIV-1_{NL4-3} is highly cytopathic and readily induces syncytia. The *nef* mutants of both isolates grew with kinetics similar to those of parental virus strains in stimulated peripheral blood lymphocytes but demonstrated attenuated growth properties in vivo. HIV-1_{NL4-3} induced severe depletion of human thymocytes within 6 weeks of infection, whereas its *nef* mutant did not. Thus, HIV-1 Nef is required for efficient in vivo viral replication and pathogenicity.

The *nef* gene is conserved among primate lentiviruses and is among the first viral genes transcribed following infection (29). This would suggest a critical role for Nef in the virus life cycle, and therefore in the pathogenesis of lentiviral infections, yet the function of Nef has not been determined. While Nef was originally defined as a negative factor and thought to down-regulate virus replication (4, 20, 26), recent data demonstrate that Nef is dispensable for both viral replication and cytopathic effects in vitro (11, 14, 17). The *nef* gene product causes down-regulation of CD4 in vitro (12, 22, 31) and in transgenic mice (32), although neither this phenomenon nor its relevance has been demonstrated in in vivo infection. In addition, Nef has been shown to be required for simian immunodeficiency virus (SIV) pathogenicity in vivo (16). The recent success utilizing *nef* deletion mutants of SIV as a live attenuated vaccine (9) emphasizes the importance of investigating the role of human immunodeficiency virus type 1 (HIV-1) Nef in in vivo replication and pathogenesis and determining if mutations in *nef* result in an attenuated phenotype in vivo.

We and others have recently shown that the SCID-hu mouse can be used as an in vivo model to study HIV-1 infection (15, 24) and pathogenicity (5, 6, 33). This model employs severe combined immunodeficient (SCID) mice (7) that are incapable of rejecting xenografts. When human fetal liver and thymus pieces are implanted under the murine kidney capsule (23), a conjoint organ forms that supports the long-term differentiation and maturation of human thymocytes (25) and, upon histological examination, resembles a normal human fetal thymus (5, 6, 23, 25, 33). Infection of the thymus and liver implants with HIV results in pathological changes in this organ, making the SCID-hu mouse the first animal model to display HIV-induced pathology in a lymphoid organ. The observed changes include severe depletion of CD4-bearing thymocytes (5, 6), loss of cortical-medullary junctions, and hypocellularity (5, 6, 33). There is some evidence of apoptosis as a mechanism for thymocyte depletion in this system (6). In addition, Stanley et al. have reported degeneration of thymic epithelial cells (33). While the kinetics and severity of pathology differ with the virus strain used (5, 6, 33), these changes are consistent with pathology observed in the thymuses of HIV-infected individuals and fetuses (13, 28). Thus, the SCID-hu mouse provides a suitable in vivo model with which to examine HIV-1 pathogenesis in lymphoid tissue and may provide conditions not available in tissue culture systems using mitogen-stimulated peripheral blood lymphocytes.

Although HIV-1 Nef is dispensable for replication and cytopathicity in vitro, its importance in HIV-1 infection in vivo remains unclear. Therefore, we have used the SCID-hu model to investigate the requirement for HIV-1 Nef for in vivo replication and pathogenicity. Our results demonstrate that in contrast to in vitro experiments, replication and pathogenicity of HIV-1 in vivo is dependent on the presence of Nef.

MATERIALS AND METHODS

Virus and cells. The *nef* mutant, HIV-$1_{JR-CSF-X}$, was generated by a frameshift at the *Xho*I site at nucleotide position 8914 of HIV-1_{JR-CSF} (18). The proviral contruct, pNL-Δnef, was constructed by deleting the first 219 nucleotides of the *nef* gene in plasmid pNL4-3 (1) as follows. By PCR mutagenesis, *Xho*I and *Mlu*I endonuclease restriction sites were introduced one nucleotide 3′ to the envelope gene stop codon and directly 5′ of the *Kpn*I site within *nef*, respectively. The 5′ coding region of *nef* was subsequently deleted by cleaving with *Xho*I and *Mlu*I and inserting a 22-bp synthetic oligonucleotide linker composed of two oligonucleotides with the sequences 5′-TCGAC TGAATTCTACGCGTTAT-3′ and 5′-CGCGATAACGCG TAGAATTCAG-3′.

All virus stocks were obtained by electroporation (8) of molecular clones (50 μg) into 10^7 COS cells. One-, two-, and three-day virus stocks were collected, filtered, and assayed for $p24^{gag}$ content by enzyme-linked immunosorbent assay (ELISA) (Coulter, Hialeah, Fla.). Virus stocks were stored at −70°C. To standardize infections, infectious units were deter-

* Corresponding author. Mailing address: Division of Hematology-Oncology, 11-934 Factor Building, Department of Medicine, UCLA School of Medicine and Jonsson Comprehensive Cancer Center, Los Angeles, CA 90024-1678. Phone: (310) 794-7765. Fax: (310) 825-6192.

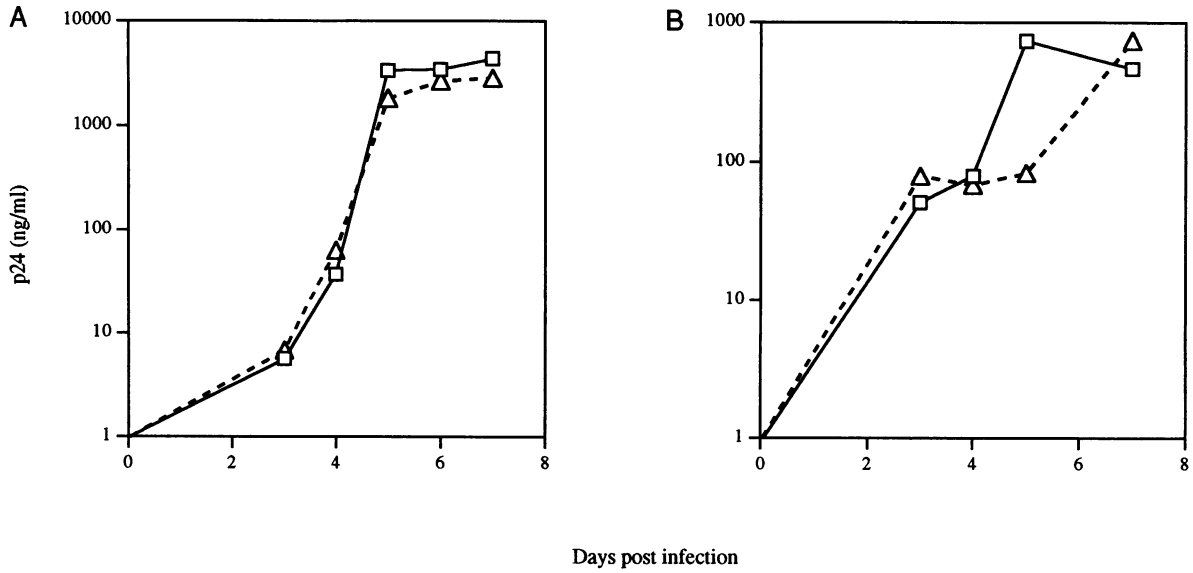

FIG. 1. In vitro replication kinetics of HIV-1 *nef* mutants. (A) HIV-1_{JR-CSF} and HIV-$1_{JR-CSF-X}$; (B) HIV-1_{NL4-3} and HIV-$1_{NL-\Delta nef}$. Squares represent wild-type virus, and triangles represent the *nef* mutants. Viral replication in phytohemagglutinin-stimulated PBMC was quantitated by ELISA for HIV-1 p24 antigen at the indicated days postinfection. In panel A, 5×10^6 PBMC were infected with approximately 10^3 IU of virus; 2.5×10^3 IU was added to 5×10^6 PBMC in panel B. Data in each were obtained from different PBMC donors.

mined by limiting dilution on phytohemagglutinin-stimulated human peripheral blood mononuclear cells (PBMC).

Human PBMC were obtained from normal donors by venipuncture or from leukopacks purchased from the American Red Cross. Peripheral blood lymphocytes were isolated by centrifugation over Ficoll-Hypaque and depleted of macrophages by plastic adherence for 72 h.

Construction and infection of SCID-hu mice. C.B-17 mice homozygous for the SCID genetic defect (7) were originally obtained from K. Dorshkin and subsequently bred at the University of California, Los Angeles. The mice were housed in a biosafety level 3 facility at the University of California, Los Angeles, in accordance with institutional guidelines. For invasive procedures, mice were anesthetized with methoxyflurene as an inhalent and a combination of ketamine HCl with xylazine injected intramuscularly (1 mg/10 g of body weight). Human fetal thymus and liver were implanted under the left kidney capsule of SCID mice 6 to 8 weeks of age as described previously (5, 6, 23, 25). Fetal tissue was obtained (Advanced Bioscience Resources, Alameda, Calif.) from individual donors ranging from 16 to 24 weeks of gestation. In Fig. 2A and 4 and Table 2, the animals are identified by numbers. The number preceding the hyphen indicates the fetal tissue donor, and the number after the hyphen represents the particular mouse. Four to eight months postimplantation, implants were injected with 200 infectious units (IU) of virus in 50-μl volumes (5). Mock implants were infected with 50 μl of supernatant from mock-electroporated COS cells.

Quantitative PCR amplification. Single-cell suspensions obtained from biopsied implants were washed once in phosphate-buffered saline (PBS), lysed in urea lysis buffer (4.7 M urea, 1.3% [wt/vol] sodium dodecyl sulfate, 0.23 M NaCl, 0.67 mM EDTA [pH 8.0], 6.7 mM Tris-HCl), and subjected to phenol-chloroform extraction and ethanol precipitation. Total nucleic acids obtained from this procedure were then subjected to quantitative PCR amplification as previously described (5, 34, 35). Briefly, 25 cycles of amplification were performed, using the ^{32}P-end-labeled M667-AA55 primer pair specific for the R/U5 region of the viral long terminal repeat. To quantitatively detect cellular DNA, primers specific for human β-globin (nucleotides 14 to 33 and 123 to 104) (19, 34) were used with 21 cycles of amplification. To generate standard curves for HIV-1 DNA, four- or fivefold dilutions were made of cloned HIV-1_{JR-CSF} DNA (8) digested with *Eco*RI, which does not cleave viral sequences. These dilutions were made into DNA from PBMC (10 μg/ml). Human β-globin standard curves were usually derived from 3-fold dilutions of PBMC DNA, except for the experiments in Fig. 2A, in which 10-fold dilutions were used. Standard curves for both HIV-1 and β-globin were amplified in parallel. For PCR analysis, nucleic acids were added to 15 μl of low-salt PCR buffer (25 mM Tris [pH 8.0], 2 mM $MgCl_2$, 30 mM NaCl, 0.1 mg of bovine serum albumin per ml, 0.25 mM deoxynucleoside triphosphate). The reaction volume was brought up to 25 μl with S/P high-purity water (Baxter Healthcare Corp., McGaw Park, Ill.).

Following amplification, radiolabeled products were resolved on a 6% polyacrylamide gel. Values were obtained by interpolation from the standard curve, using an Ambis radioanalytic imager (Ambis, San Diego, Calif.).

Flow cytometry. Thymocyte subset distribution was determined by flow cytometry. Single-cell suspensions obtained from biopsy samples were washed once in PBS, and then 10^6 cells were costained with monoclonal antibodies (MAbs) (Becton Dickinson, Mountain View, Calif.) to CD4 and CD8 T-cell markers. Anti-CD4 was fluorescein isothiocyanate conjugated. Staining with the biotinylated anti-CD8 was followed with avidin-allophycocyanin. As a positive control, normal human peripheral blood was stained with anti-CD4 and anti-CD8 MAbs. An anti-mouse immunoglobulin G1 MAb was used at all time points to stain peripheral blood as an isotype control. After staining, erythrocytes were lysed by incubation in fluorescence-activated cell sorting lysing solution (Becton Dickinson). Cells were then fixed in 2% paraformaldehyde. Data were accumulated on a FACStar^{Plus} flow cytometer and analyzed with the Lysis II program (Becton Dickinson). Forward-versus-side scatter analysis of mock-infected implants was used

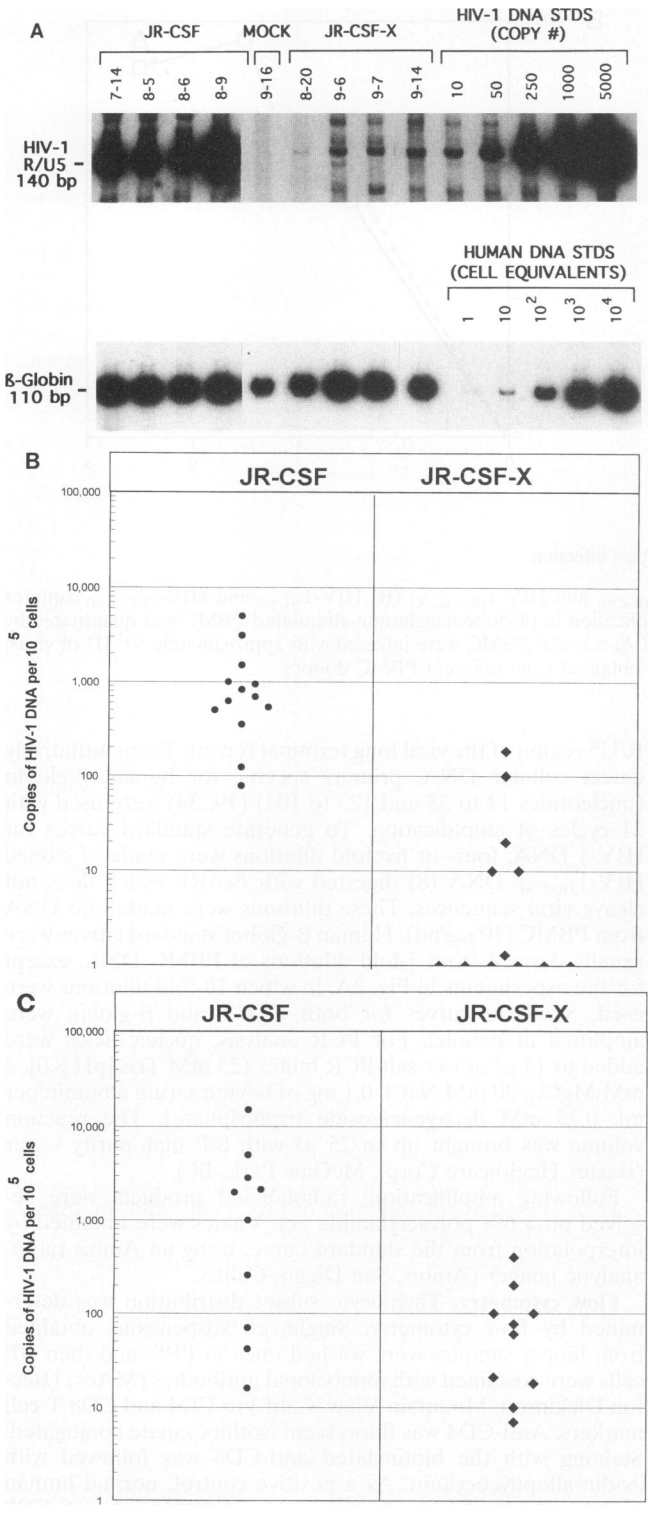

FIG. 2. In vivo replication of HIV-$1_{JR\text{-}CSF\text{-}X}$. The number of HIV-1 genomes in 10^5 human thymocytes was determined in implants 3 to 4 (A and B) and 6 (C) weeks postinfection. (A) PCR data for four HIV-$1_{JR\text{-}CSF}$-infected animals, four HIV-$1_{JR\text{-}CSF\text{-}X}$-infected animals, and one mock-infected animal. Replicate samples were analyzed for human β-globin sequences (bottom panel), allowing quantitation of viral genomes per human cell equivalent. Signals from quantitative HIV-1 DNA and cellular DNA standards assayed in parallel are shown at the right of each panel. (B and C) Summary of PCR data for 3 to 4 (B) and 6 (C) weeks postinfection. The differences in virus load between mutant and wild type were statistically significant (Wilcoxon rank sum test; 3 weeks, $P = 0.0001$; 6 weeks, $P = 0.028$).

to gate on the live thymocyte population. A total of 5×10^3 to 10×10^3 events were acquired, except from implants severely depleted of CD4-bearing thymocytes.

RESULTS

Replication of HIV-1 wild-type and *nef* mutants. To investigate the in vivo requirement for HIV-1 Nef, SCID-hu mice were constructed by implanting human fetal thymus and liver under the kidney capsule (5, 6, 23, 25) of SCID mice (7). Four to six months following implantation, the human thymus and liver implants were inoculated with 200 IU of one of either of two different wild-type isolates of HIV-1 or their *nef* mutants: HIV-$1_{JR\text{-}CSF}$ (18) or a *nef* frameshift mutant of HIV-$1_{JR\text{-}CSF}$ (HIV-$1_{JR\text{-}CSF\text{-}X}$), or HIV-$1_{NL4\text{-}3}$ (1) or a *nef* deletion mutant of this isolate (HIV-$1_{NL\text{-}\Delta nef}$). These two parental viruses differ in their in vitro phenotypes in that HIV-$1_{JR\text{-}CSF}$ is relatively noncytopathic and does not induce syncytia, whereas HIV-$1_{NL4\text{-}3}$ readily induces syncytia. As reported for *nef* mutants of other HIV-1 molecular clones (14, 17), the *nef* mutants used in these studies show in vitro growth kinetics in mitogen-stimulated PBMC cultures similar to those of the parental strains (Fig. 1). The in vitro syncytium-inducing phenotype of HIV-$1_{NL4\text{-}3}$ was also not affected by the *nef* deletion (data not shown).

Implants infected with either HIV-$1_{JR\text{-}CSF}$ or HIV-$1_{JR\text{-}CSF\text{-}X}$ were subjected to sequential biopsies of approximately 25% of the human organ at 3 to 4 weeks and again at 6 weeks postinfection and analyzed for viral DNA by quantitative PCR (5, 34, 35). An example of this analysis at the 3- to 4-week time point is illustrated in Fig. 2A. Implants infected with HIV-$1_{JR\text{-}CSF}$ contained an average of ≈1,200 copies of viral DNA per 10^5 human cells, while the implants infected with HIV-$1_{JR\text{-}CSF\text{-}X}$ contained an average of ≈30 copies per 10^5 cells. Thus, there was an approximately 40-fold difference in the ability of these viruses to replicate at this time point (Fig. 2B). By the 6-week time point, average wild-type HIV-$1_{JR\text{-}CSF}$ virus load increased approximately twofold to ≈2,800 copies of viral DNA per 10^5 human cells, while implants infected with its *nef* mutant demonstrated an approximately threefold increase in viral load. Thus, at 6 weeks postinfection, an average of ≈100 copies of HIV-1 DNA per 10^5 cells were recovered from implants infected with the mutant virus, resulting in an approximately 30-fold difference in genome number between these two viruses (Fig. 2C).

HIV-$1_{NL4\text{-}3}$ replicates more rapidly than HIV-$1_{JR\text{-}CSF}$ in this system, such that infected implants contained an average of approximately 1,800 copies of HIV-1 DNA per 10^5 cells at 3 weeks postinfection. However, at this time point, viral DNA was undetectable in implants infected with HIV-$1_{NL\text{-}\Delta nef}$ (Fig. 3A). The inability to detect viral DNA in these implants was most likely due to sensitivity of the assay, since estimated initial multiplicities of infection were approximately 1 IU/5×10^5 cells. Because of severe thymocyte depletion at 6 weeks postinfection (Tables 1 and 2), only four of eight implants infected with HIV-$1_{NL4\text{-}3}$ yielded sufficient numbers of human thymocytes to analyze by PCR. The average copy number of HIV-1 DNA had increased to approximately 13,000 copies per 10^5 cells at the 6-week time point (Fig. 3B). Low copy numbers of HIV-1 DNA (average of eight copies per 10^5 cells) were

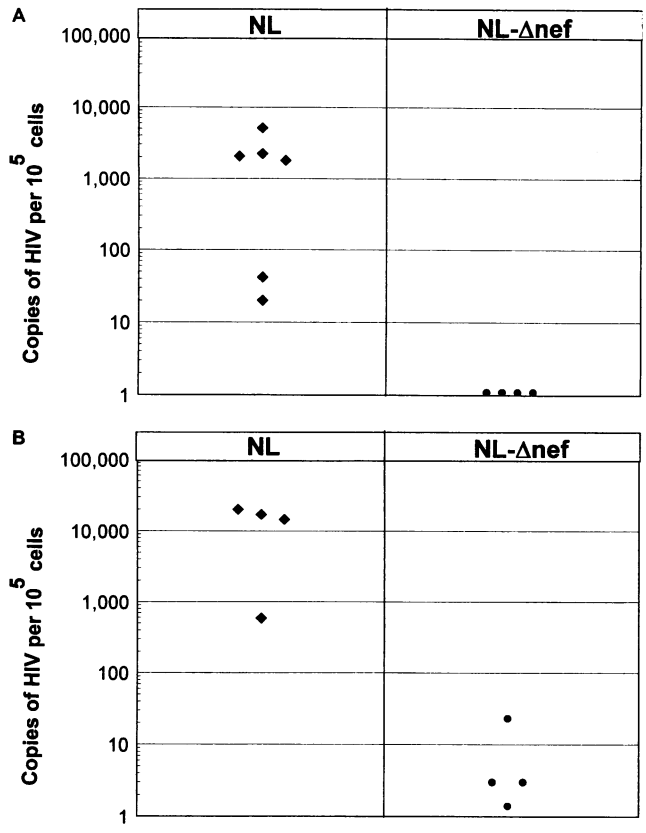

FIG. 3. In vivo replication of HIV-$1_{NL\text{-}\Delta nef}$. Shown are copies of HIV-1 genomes per 10^5 thymocytes 3 (A) and 6 (B) weeks postinfection. HIV-$1_{NL4\text{-}3}$ or HIV-$1_{NL\text{-}\Delta nef}$ (200 IU) was injected into thymus and liver implants derived from fetal donors 17 to 24 weeks of gestational age. All implants were sequentially biopsied at the indicated times and analyzed for HIV-1 genomes and human β-globin as described previously (5, 34, 35). Points positioned on the baseline indicate undetectable viral DNA. The differences in virus load between these mutant and wild-type strains were significant at both time points (3 weeks, $P = 0.011$; 6 weeks, $P = 0.03$).

detected at this time point in HIV-$1_{NL\text{-}\Delta nef}$-infected implants, confirming that mutant virus was introduced and remained viable in vivo. A single implant (14-26) infected with HIV-$1_{NL\text{-}\Delta nef}$ was subsequently analyzed at 12 weeks postinfection and contained ≈700 copies of HIV-1 DNA per 10^5 cells (data not shown). PCR analysis of the viral *nef* gene in thymocyte DNA from this time point demonstrated the presence of the deletion, establishing that this viral DNA was due to replication of the mutant virus and not to selective outgrowth of a low-level wild-type contaminant (data not shown). These results demonstrate that while the *nef* mutants of both of these parental viruses are replication competent, they are growth attenuated in vivo.

Pathogenicity of viruses in vivo. To determine if thymocytes were depleted as a result of HIV-1 infection, all implants were analyzed by two-color flow cytometry for human CD4 and CD8. No depletion of $CD4^+$ human thymocytes was observed in implants infected with either HIV-$1_{JR\text{-}CSF}$ or its *nef* mutant at 3 or 6 weeks postinfection compared with controls consisting of mock-infected implants (data not shown). At 9 weeks postinfection, one of five HIV-$1_{JR\text{-}CSF}$-infected implants was depleted of both mature and immature CD4-bearing thymocytes. No depletion was seen in the four implants infected with HIV-$1_{JR\text{-}CSF\text{-}X}$ (data not shown). We and others previously demonstrated that the HIV-$1_{JR\text{-}CSF}$ isolate depletes thymocytes in vivo less efficiently than some other viral isolates (5, 6, 33). Consequently, we analyzed eight implants infected with the HIV-$1_{NL4\text{-}3}$ isolate, which is more cytopathic than the HIV-$1_{JR\text{-}CSF}$ isolate both in vitro and in vivo. These implants appeared normal at 3 weeks postinfection, demonstrating approximately 75 to 85% $CD4^+$ $CD8^+$ cells, with the majority of the remaining cells being positive for either CD4 or CD8 (Fig. 4). However, by 6 weeks postinfection, all eight HIV-$1_{NL4\text{-}3}$-infected implants demonstrated severe depletion of CD4-bearing thymocytes (Fig. 4; Tables 1 and 2). Both immature CD4 CD8 double-positive and mature $CD4^+$ $CD8^-$ thymocytes were depleted, resulting in a relative increase of $CD4^-$ $CD8^+$ and $CD4^-$ $CD8^-$ thymocytes. Some depletion of the $CD4^-$ $CD8^+$ T-cell subset was observed in one implant (16-9) (Table 2). By histological analysis, all eight of these implants demonstrated depletion of cortical thymocytes, similar to that previously described (references 5 and 6 and data not shown). When analyzed at 9 weeks postinfection, three of four HIV-$1_{NL4\text{-}3}$-infected implants clearly remained depleted of CD4-bearing thymocytes. In addition, implant 11-8, although depleted of thymocytes (by histological analysis), displayed reemergence of $CD4^+$ thymocytes when assessed by flow cytometry. We and others have previously observed a decrease in virus load following the depletion of CD4-bearing thymocytes in thymus and liver implants (5, 6). It is possible that the depleted thymus, in the presence of lesser amounts of virus, retains the ability to support regeneration of new thymocytes. Therefore, the observed reemergence of $CD4^+$ thymocytes in implant 11-8 may reflect a dynamic interaction between infection and depletion of target cells and the regeneration of new thymocytes.

In contrast to HIV-$1_{NL4\text{-}3}$-infected implants, depletion of CD4-bearing thymocytes was not observed in any of the five HIV-$1_{NL\text{-}\Delta nef}$-infected implants by 6 weeks postinfection (Fig. 4; Tables 1 and 2). Histological analysis revealed that these implants all had normal cortical and medullary regions (data

TABLE 1. Summary of thymocyte subset distribution in mock-, HIV-$1_{NL4\text{-}3}$-, and HIV-$1_{NL\text{-}\Delta nef}$-infected implants[a]

Infection	%							
	3 wk postinfection				6 wk postinfection			
	$CD4^+$	$CD4^+$ $CD8^+$	$CD4^-$ $CD8^-$	$CD8^+$	$CD4^+$	$CD4^+$ $CD8^+$	$CD4^-$ $CD8^-$	$CD8^+$
Mock	15.3 ± 10.9	76.1 ± 13.9	3.1 ± 2.0	5.3 ± 2.9	14.7 ± 7.1	67.7 ± 12.4	8.3 ± 5.7	9.2 ± 6.9
HIV-$1_{NL4\text{-}3}$	8.6 ± 3.0	81.5 ± 4.5	3.4 ± 0.7	6.3 ± 2.0	16.2 ± 11.1	3.0 ± 5.6	43.4 ± 30.8	37.3 ± 23.7
HIV-$1_{NL\text{-}\Delta nef}$	8.2 ± 3.0	84.1 ± 4.4	3.0 ± 0.8	4.4 ± 1.2	7.0 ± 3.8	71.3 ± 17.6	16.2 ± 12.9	5.3 ± 3.2

[a] Thymocytes from implants infected as indicated were analyzed for CD4 and CD8 surface markers. Quadrants were selected as shown in Fig. 4. Mock-infected implants were assayed in parallel with the experimental implants. Values are averages ± standard deviations of the individual values shown in Table 2.

TABLE 2. Thymocyte subset distribution in individual implants[a]

Infection	Mouse	%											
		3 wk postinfection				6 wk postinfection				9 wk postinfection			
		$CD4^+$	$CD4^+$ $CD8^+$	$CD4^-$ $CD8^-$	$CD8^+$	$CD4^+$	$CD4^+$ $CD8^+$	$CD4^-$ $CD8^-$	$CD8^+$	$CD4^+$	$CD4^+$ $CD8^+$	$CD4^-$ $CD8^-$	$CD8^+$
Mock	9-16[b]	NT	NT	NT	NT	20.9	63.7	2.5	12.7				
	10-1[b,c]	31.7	48.3	7.7	12.3	13.3	71.3	8.1	7.3				
	10-10[c]	28.7	65.7	1.7	3.9	15.1	63.9	17.5	3.5	7.6	80.9	6.8	4.6
	11-17[b,c]	24.4	69.8	1.5	4.3	17.4	71.7	2.1	8.8				
	12-16	NT	NT	NT	NT	7.0	66.4	12.8	13.7	6.2	87.6	2.5	3.6
	14-1[b,c]	6.3	86.3	2.8	4.4	8.2	72.7	15.2	3.7				
	14-3	NT	NT	NT	NT	15.6	71.8	7.0	5.4				
	14-4[b,c]	9.7	80.9	3.9	5.4	28.3	40.5	6.8	24.3				
	14-9[c]	7.5	86.8	2.5	3.0	6.6	87.2	2.9	3.1	12.3	81.0	3.2	3.4
	16-14[c]	7.5	86.6	2.0	3.7	NT	NT	NT	NT	17.5	70.2	2.2	9.9
	17-1	7.0	84.7	2.5	5.5	NT	NT	NT	NT	10.1	81.3	5.3	3.1
HIV_{NL4-3}	11-4[b]	NT	NT	NT	NT	29.3	1.0	4.6	65.0				
	11-8	NT	NT	NT	NT	31.1	1.8	15.3	51.6	6.3	50.3	39.4	3.0
	11-10[b]	NT	NT	NT	NT	3.0	0.4	55.5	40.9				
	11-11[b]	NT	NT	NT	NT	13.7	0.8	41.4	43.9				
	14-6[c]	6.7	85.2	3.6	4.4	21.0	1.1	61.8	16.6				
	14-10[c]	12.3	78.7	2.5	6.3	19.0	1.7	15.3	63.8	2.9	5.6	78.6	12.7
	16-2[c]	5.7	85.5	3.1	5.4	11.6	16.8	55.8	15.5	11.8	2.8	39.0	46.2
	16-9[a,b]	9.9	76.7	4.2	9.1	0.8	0.4	97.5	1.1	2.7	1.0	90.1	6.0
$HIV_{NL-\Delta nef}$	14-16	8.8	83.8	2.8	4.4	4.9	86.7	5.2	3.1	9.8	75.9	13.2	0.9
	14-26	6.1	87.3	2.2	4.2	5.4	80.9	9.2	4.3	17.8	69.7	6.5	5.9
	14-29[b]	6.3	87.3	2.6	3.5	13.7	52.8	23.1	10.3				
	16-13	13.2	76.7	3.5	6.4	6.1	51.7	35.6	6.5	19.8	15.4	43.9	20.7
	16-16[b]	6.5	85.6	4.1	3.7	5.1	84.6	7.7	2.4				

[a] Thymocyte subsets were determined as described for Table 1. Values shown for the 3- and 6-week time points are for the individual implants summarized in Table 1. NT, not tested.

[b] Sacrificed prior to the 9-week biopsy.

[c] Data obtained at the 3- and 6-week time points were previously published (5).

not shown). One of three HIV-$1_{NL-\Delta nef}$-infected implants (16-13) tested at 9 weeks postinfection exhibited minor depletion of $CD4^+$ thymocytes (Table 1). However, virus load was not assessed at this time point. The only HIV-$1_{NL-\Delta nef}$-infected implant tested at 12 weeks postinfection (implant 14-26) exhibited no $CD4^+$ thymocyte depletion (data not shown). The results of the flow cytometric analysis demonstrate that the pathogenic nature of HIV-1_{NL4-3} is severely attenuated by inactivation of the *nef* gene.

DISCUSSION

Our results demonstrate that the *nef* mutants of two phenotypically distinct HIV-1 strains are replication competent yet attenuated for growth and cytopathicity in vivo. Thus, the *nef* gene is required for efficient in vivo replication and pathogenicity of HIV-1. The in vivo system presented here may provide a means to determine the function of Nef. In the rhesus macaque, introduction of SIV *nef* mutants results in inefficient virus replication, lack of disease progression, and generation of a protective immune response (9, 16). One interpretation of these data is that SIV *nef* mutants are intrinsically more immunogenic or less able to escape the immune response. However, the attenuation of the HIV-1 *nef* mutants in SCID-hu mice occurs most likely in the absence of an immune response. SCID mice lack functional T and B cells, as they cannot rearrange immunoglobulin or T-cell receptor genes (21, 30). In addition, it is unlikely that the differentiating human thymocytes in these animals generate an effective anti-HIV response in the human implant. Therefore, attenuation of the *nef* mutants is most likely due to an alteration of the interaction between HIV and its target cell.

One interaction of the *nef* gene with $CD4^+$ T cells that has been documented in vitro is Nef-induced down-regulation of surface CD4 (12, 22, 31). No down-regulation of CD4 was observed in our in vivo system in thymocytes infected with either of the two HIV strains or their *nef* mutants, as measured by intensity of CD4 staining using flow cytometry (Fig. 4 and data not shown). It is possible that CD4 down-regulation may not have been detectable at the 3- or 6-week time point, as, at most, only ≈15% of thymocytes were infected. However, down-regulation of CD4 is not responsible for the observed loss of $CD4^+$ thymocytes in implants infected with HIV, as histological and flow cytometric analyses of infected implants show atrophy and severe hypocellularity (5, 6, 33), reflecting a significant loss of cell numbers.

The lower viral burden in implants infected with *nef* mutants demonstrates that Nef is required for the efficient replication of virus in thymocytes. The relationship between high virus load and cell depletion in implants infected with HIV-1_{NL4-3} suggests that the decrease in pathogenicity of the *nef* mutants is related to viral replication. The dichotomy between in vitro systems, in which Nef appears to be dispensable for virus replication, and this in vivo model, in which *nef* mutants display attenuated replication, suggests that insight into the mechanism of Nef action may be found in the differences between the two models themselves. One difference between the two systems is the target cell type. Most in vitro systems utilize terminally differentiated, actively replicating T lymphocytes. Thymocytes, however, are undergoing differentiation, and only a relatively low percentage (10 to 20%) (data not shown) are traversing the cell cycle at any given time. The function of Nef may therefore be related to the difference in the activation/differentiation state of these two target cell types. Early

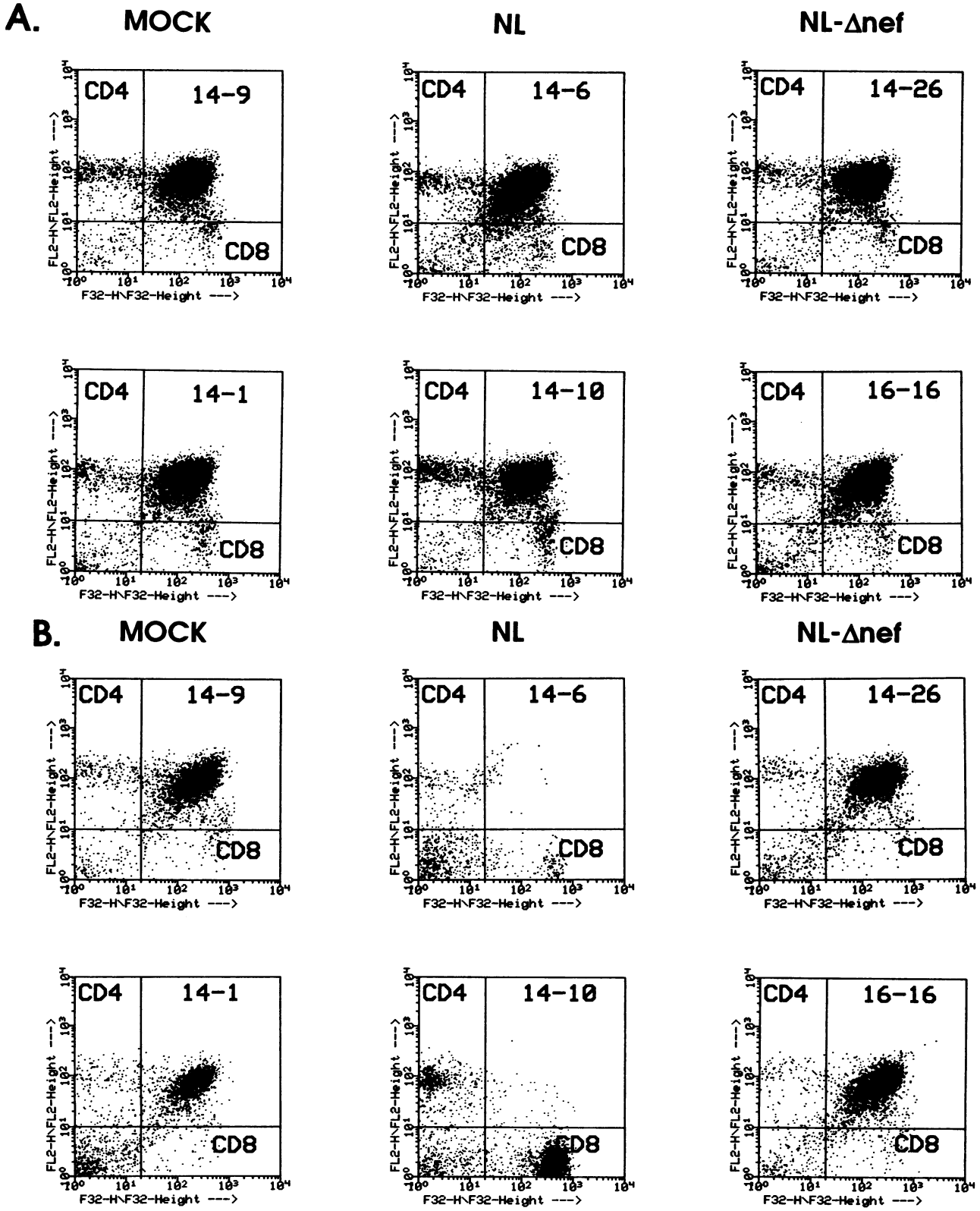

FIG. 4. Flow cytometric analysis of HIV-1_{NL4-3}- and HIV-$1_{NL-\Delta nef}$-infected implants. Implants were infected with 200 IU of the indicated virus or with 50 μl of supernatant from mock-electroporated cells. Thymocytes were analyzed for CD4 and CD8 surface antigens by two-color flow cytometry at 3 (A) and 6 (B) weeks postinfection. Dot plots from two representative implants are shown for each group: mock-, HIV-1_{NL4-3}-, and HIV-$1_{NL-\Delta nef}$-infected implants.

studies, although controversial, suggested that Nef negatively influences the transcription of HIV by interacting with cellular factors (4, 20). In contrast to those studies, our results demonstrate that *nef* mutants do not replicate as well as wild-type HIV-1 in differentiating thymocytes. It is conceivable that Nef positively influences the expression of HIV-1 in this cell type. Studies using the SCID-hu model are currently under way in this laboratory to determine the mechanism(s) responsible for the attenuated replication by *nef* mutants as well as to define the regions of Nef critical for its function in vivo.

Our results indicate that Nef is required for optimal growth and cytopathic properties of HIV-1 in the human thymus in vivo. These results are in agreement with previously published work in the SIV system (9, 16) and suggest that the attenuated properties of SIV *nef* mutants are likely due to inefficient replication in lymphoid tissues. This inefficient replication could allow for appropriate antigen presentation and immune activation before significant depletion of lymphocytes occurs, resulting in host control of the virus and protective immunity. Poor replication in lymphoid tissues and an effective immune response could also prevent virus from becoming sequestered in lymphoid tissues which, in HIV-infected humans, have been shown to act as a reservoir of viral particles and viral antigens during the clinical latency period (10, 27).

Administration of *nef* deletion mutants of SIV to rhesus macaques appears to be the most effective method of antilentivirus vaccination to date (9). However, since SIV and HIV-1 are not genetically identical, absolute parallels between these two viruses cannot be drawn. The SCID-hu model is the only animal model currently available in which HIV-1-induced pathology can be demonstrated (5, 6, 33). Our results suggest that the SCID-hu mouse may be a useful model for quantitatively assessing the pathogenic properties of candidates for live attenuated HIV-1 vaccine strains. By using this system, it may be possible to identify mutations in other accessory genes, individually or in combination with *nef* mutations, which may result in a more attenuated phenotype. This type of assessment is not possible in immunocompetent primate models, in which the host immune response may affect viral replication. However, because the best test of vaccine potential is the ability of the immune response to control both replication and pathogenicity, studies in SCID-hu mice would be complemented by studies involving infection of immunocompetent animals such as chimpanzees (3) or pigtailed macaques (2) to determine if the altered viruses would be able to evoke immune responses. This type of coordinated research effort may provide an approach for preclinical assessment of live attenuated HIV-1 vaccine strains.

ACKNOWLEDGMENTS

We thank Gerold Feuer and Rafi Ahmed for discussion and critical review of the manuscript.

This work was supported by the UC Universitywide AIDS Research Program, the UCLA CFAR (NIH), the McCarthy Family Foundation, and a gift from Jim Bridger for the initiation of the SCID mouse P3 facility. G.M.A. is a Pediatric AIDS Foundation Scholar.

REFERENCES

1. **Adachi, A., H. E. Gendelman, S. Koenig, T. Folks, R. Willey, A. Rabson, and M. A. Martin.** 1986. Production of acquired immunodeficiency syndrome-associated retrovirus in human and nonhuman cells transfected with an infectious molecular clone. J. Virol. **59:**284–291.
2. **Agy, M. B., L. R. Frumkin, L. Corey, R. W. Coombs, S. M. Wolinsky, J. Koehler, W. R. Morton, and M. G. Katze.** 1992. Infection of Macaca nemestrina by human immunodeficiency virus type-1. Science **257:**103–106.
3. **Alter, H. J., J. W. Eichberg, H. Masur, W. C. Saxinger, R. Gallo, A. M. Macher, H. C. Lane, and A. S. Fauci.** 1984. Transmission of HTLV-III infection from human plasma to chimpanzees: an animal model for AIDS. Science **226:**549–552.
4. **Ahmad, N., and S. Venkatesan.** 1988. *Nef* protein of HIV-1 is a transcriptional repressor of HIV-1 LTR. Science **241:**1481–1485.
5. **Aldrovandi, G. M., G. Feuer, L. Gao, B. Jamieson, M. Kristeva, I. S. Y. Chen, and J. A. Zack.** 1993. The SCID-hu mouse as a model for HIV-1 infection. Nature (London) **363:**732–736.
6. **Bonyhadi, M. L., L. Rabin, S. Salimi, D. A. Brown, J. Kosek, J. M. McCune, and H. Kaneshima.** 1993. HIV induces thymus depletion in vivo. Nature (London) **363:**728–736.
7. **Bosma, G. C., R. P. Custer, and M. J. Bosma.** 1983. A severe combined immunodeficiency mutation in the mouse. Nature (London) **301:**527–530.
8. **Cann, A. J., Y. Koyanagi, and I. S. Y. Chen.** 1988. High efficiency transfection of primary human lymphocytes and studies of gene expression. Oncogene **3:**123–128.
9. **Daniel, M. D., F. Kirchoff, S. C. Czajak, P. K. Sehgal, and R. C. Desrosiers.** 1992. Protective effects of a live attenuated SIV vaccine with a deletion in the *nef* gene. Science **258:**1938–1941.
10. **Embretson, J., M. Zupancic, J. L. Ribas, A. Burke, P. Racz, K. Tenner-Racz, and A. T. Haase.** 1993. Massive covert infection of helper T lymphocytes and macrophages by HIV during the incubation period of AIDS. Nature (London) **362:**359–362.
11. **Fisher, A. G., L. Ratner, H. Mitsuya, L. M. Marselle, M. E. Harper, S. Broder, R. C. Gallo, and F. Wong-Staal.** 1986. Infectious mutants of HTLV-III with changes in the 3′ region and markedly reduced cytopathic effects. Science **233:**655–659.
12. **Garcia, J. V., and A. D. Miller.** 1991. Serine phosphorylation-independent downregulation of cell-surface CD4 by *nef*. Nature (London) **350:**508–511.
13. **Grody, W. W., S. Fligiel, and F. Naeim.** 1985. Thymus involution in the acquired immunodeficiency syndrome. Am. J. Clin. Pathol. **84:**85–95.
14. **Hammes, S. R., E. P. Dixon, M. H. Malim, B. R. Cullen, and W. C. Greene.** 1989. Nef protein of human immunodeficiency virus type 1: evidence against its role as a transcriptional inhibitor. Proc. Natl. Acad. Sci. USA **86:**9549–9553.
15. **Kaneshima, H., C.-C. Shih, R. Namikawa, L. Rabin, H. Outzen, S. G. Machado, and J. M. McCune.** 1991. Human immunodeficiency virus infection of human lymph nodes in the SCID-hu mouse. Proc. Natl. Acad. Sci. USA **88:**4523–4527.
16. **Kestler, H. W., III, D. J. Ringler, K. Mori, D. L. Panicali, P. K. Sehgal, M. D. Daniel, and R. C. Desrosiers.** 1991. Importance of the *nef* gene for maintenance of high virus loads and for development of AIDS. Cell **65:**651–662.
17. **Kim, S., K. Ikeuchi, R. Byrn, J. Groopman, and D. Baltimore.** 1989. Lack of a negative influence on viral growth by the *nef* gene of human immunodeficiency virus type 1. Proc. Natl. Acad. Sci. USA **86:**9544–9548.
18. **Koyanagi, Y., S. Miles, R. T. Mitsuyasu, J. E. Merrill, H. V. Vinters, and I. S. Y. Chen.** 1987. Dual infection of the central nervous system by AIDS viruses with distinct cellular tropisms. Science **236:**819–822.
19. **Lawn, R. M., A. Efstratindus, C. O'Connell, and T. Maniatis.** 1980. The nucleotide sequence of the human β-globin gene. Cell **21:**647–651.
20. **Luciw, P. A., C. Cheng-Mayer, and J. A. Levy.** 1987. Mutational analysis of the human immunodeficiency virus: the *orf*-B region down-regulates virus replication. Proc. Natl. Acad. Sci. USA **84:**1434–1438.
21. **Malynn, B. A., T. K. Blackwell, G. M. Fulop, G. A. Rathbun, A. J. W. Furley, P. Ferrier, L. B. Heinke, R. A. Phillips, G. D. Yancopoulos, and F. W. Alt.** 1988. The *scid* defect affects the final step of the immunoglobulin VDJ recombinase mechanism. Cell **54:**453–460.
22. **Mariani, R., and J. Skowronski.** 1993. CD4 downregulation by *nef* alleles isolated from HIV-1 infected individuals. Proc. Natl. Acad. Sci. USA **90:**5549–5553.
23. **McCune, J. M., R. Namikawa, H. Kaneshima, L. D. Shultz, M. Lieberman, and I. L. Weissman.** 1988. The SCID-hu mouse: murine model for the analysis of human hematolymphoid differ-

entiation and function. Science **241:**1632–1639.
24. **Namikawa, R., H. Kaneshima, M. Lieberman, I. L. Weissman, and J. M. McCune.** 1988. Infection of the SCID-hu mouse by HIV-1. Science **242:**1684–1686.
25. **Namikawa, R., K. N. Weilbaecher, H. Kaneshima, E. J. Yee, and J. M. McCune.** 1990. Long-term human hematopoiesis in the SCID-hu mouse. J. Exp. Med. **172:**1055–1063.
26. **Niederman, T. M. J., B. J. Thielan, and L. Ratner.** 1989. Human immunodeficiency virus type 1 negative factor is a transcriptional silencer. Proc. Natl. Acad. Sci. USA **86:**1128–1132.
27. **Pantaleo, G., C. Graziosi, J. F. Demarest, L. Butini, M. Montroni, C. H. Fox, J. M. Orenstein, D. P. Kotler, and A. S. Fauci.** 1993. HIV infection is active and progressive in lymphoid tissue during the clinically latent stage of disease. Nature (London) **362:**355–358.
28. **Papiernik, M., Y. Brossard, N. Mulliez, J. Roume, C. Brechot, F. Barin, A. Goudeau, J.-F. Bach, C. Griscelli, R. Henrion, and R. Vazeux.** 1992. Thymic abnormalities in fetuses aborted from human immunodeficiency virus type 1 seropositive women. Pediatrics **89:**297–301.
29. **Robert-Guroff, M., M. Popovic, S. Gartner, P. Markham, R. C. Gallo, and M. S. Reitz.** 1990. Structure and expression of *tat*-, *rev*-, and *nef*-specific transcripts of human immunodeficiency virus type 1 in infected lymphocytes and macrophages. J. Virol. **64:**3391–3398.
30. **Schuler, W., I. J. Weiler, A. Schuler, R. A. Phillips, N. Rosenberg, T. W. Mak, J. F. Kearney, R. P. Perry, and M. J. Bosma.** 1986. Rearrangement of antigen receptor genes is defective in mice with severe combined immunodeficiency. Cell **46:**963–972.
31. **Schwartz, O., Y. Riviere, J.-M. Heard, and O. Danos.** 1993. Reduced cell surface expression of processed human immunodeficiency virus type 1 envelope glycoprotein in the presence of Nef. J. Virol. **67:**3274–3280.
32. **Skowronski, J., D. Parks, and R. Mariani.** 1993. Altered T cell activation and development in transgenic mice expressing the HIV-1 *nef* gene. EMBO J. **12:**703–713.
33. **Stanley, S. K., J. M. McCune, H. Kaneshima, J. S. Justement, M. Sullivan, E. Boone, M. Baseler, J. Adelsberger, M. Bonyhadi, J. Orenstein, C. H. Fox, and A. S. Fauci.** 1993. Human immunodeficiency virus infection of the human thymus and disruption of the thymic microenvironment in the SCID-hu mouse. J. Exp. Med. **178:**1151–1163.
34. **Zack, J. A., S. J. Arrigo, S. R. Weitsman, A. S. Go, A. Haislip, and I. S. Y. Chen.** 1990. HIV-1 entry into quiescent primary lymphocytes: molecular analysis reveals a labile, latent viral structure. Cell **61:**213–222.
35. **Zack, J. A., A. M. Haislip, P. Krogstad, and I. S. Y. Chen.** 1992. Incompletely reverse transcribed human immunodeficiency virus type 1 genomes in quiescent cells can function as intermediates in the retrovirus life cycle. J. Virol. **66:**1717–1725.